NT-pro-BNP Level is Related to Left Ventricular Remodeling in Patients With Primary Aldosteronism

Authors
Tao Wu[1‡], Chenxiao Xu[2‡], Lu Tang[1], Xi Wu[3], Pengfei Peng[1], Xun Yue[3], Wei Cheng[1], Shuai He[1], Lei Li[1], Yucheng Chen[4], Yan Ren[2], Jiayu Sun[1]

Affiliations
1 Department of Radiology, West China Hospital, Sichuan University
2 Department of Endocrinology and Metabolism, West China Hospital, Sichuan University
3 North Sichuan Medical College
4 Cardiology Division, West China Hospital, Sichuan University

Keywords
primary aldosteronism , cardiac magnetic resonance imaging, NT-pro-BNP, left ventricular remodeling

received 08.03.2024
revised 01.05.2024
accepted 03.06.2024
published online 2024

Bibliography
Exp Clin Endocrinol Diabetes
DOI 10.1055/a-2348-4468
ISSN 0947-7349

Georg Thieme Verlag KG, Rüdigerstraße 14,
70469 Stuttgart, Germany

Correspondence
Jiayu Sun
Guoxue Xiang No. 37
610041 Chengdu, Sichuan Province
People's Republic of China
Tel.: + 86-18980606253
cardiac_wchscu@163.com

Supplementary Material is available under https://doi.org/10.1055/a-2348-4468

ABSTRACT

Aims To assess the relationship between the left ventricular remodeling parameters of cardiac magnetic resonance and NT-pro-BNP in patients with primary aldosteronism (PA).

Methods Seventy-four PA and 39 essential hypertension patients were prospectively recruited and underwent cardiac magnetic resonance. Plasma NT-pro-BNP was measured before patients underwent cardiac magnetic resonance. Left ventricular remodeling parameters were defined as left ventricular function parameters, T1 mapping parameters, and strain parameters. Differences in continuous variables between two groups were analyzed using Student's t-test or Mann–Whitney U test. Differences in categorical variables between two groups were analyzed by chi-squared test. Spearman's correlation and linear regression were used to analyze the relationships between left ventricular remodeling parameters and plasma NT-Pro-BNP level. $P < 0.05$ was considered as statistically significant.

Results Patients with PA demonstrated higher NT-pro-BNP [86.0 (49.5, 145.5) vs. 45.0 (28.5, 73.5) pg/mL, $P = 0.001$] and Native T1 (1227 ± 41 vs. 1206 ± 43 ms, $P = 0.015$) level than essential hypertension patients. Compared to patients with normal NT-pro-BNP levels, those with abnormal levels demonstrated different left ventricular remodeling parameters. NT-pro-BNP level was independently related to native T1 ($\beta = 0.316$, $P = 0.006$), extracellular volume ($\beta = 0.419$, $P < 0.001$), short-axis global circumferential strain ($\beta = 0.429$, $P < 0.001$), four-chamber global longitudinal strain ($\beta = 0.332$, $P = 0.002$), and four-chamber global radial strain ($\beta = -0.334$, $P = 0.004$) in patients after adjusting for baseline characteristics.

Conclusions NT-pro-BNP level was related to left ventricular remodeling parameters derived from cardiac magnetic resonance in patients with PA. This result implies that clinicians should pay attention to NT-pro-BNP assessment in patients with PA in routine clinical assessment.

Introduction

Primary aldosteronism (PA) is a common form of secondary hypertension, which is characterized by the production of

‡ Tao Wu and Chenxiao Xu contributed equally to this paper.

excessive aldosterone and low levels of plasma renin [1]. Such inappropriate production of aldosterone can cause hypertension, cardiovascular damage, plasma renin suppression, and hypokalemia, which may lead to left ventricular remodeling [2, 3]. Left ventricular remodeling was described as compensation of the left ventricle in response to increasing cardiac preload and afterload [4]. Clinical studies have demonstrated that patients with PA had more obvious left ventricular remodeling, including increased left ventricular mass and cardiac fibrosis level, than those with essential hypertension (EH) [3, 5–7]. With the development of cardiac magnetic resonance imaging (MRI), left ventricular remodeling could be evaluated by multiple parameters, including volume, mass, function, strain, and even tissue characteristics, measured by the T1 mapping technique [8–10].

Pro B-type natriuretic peptide (pro-BNP) is synthesized in cardiomyocytes as a pre-hormone in response to increasing ventricular wall strain. Then, pro-BNP is cleaved into the biologically active brain natriuretic peptide (BNP) hormone and the biologically inactive N-terminal pro-brain natriuretic peptide (NT-pro-BNP) hormone. NT-pro-BNP is a well-established plasma biomarker of heart failure, with a longer half-life, better *in vitro* stability, and relatively higher blood concentration than BNP, another commonly used plasma biomarker of heart failure [11, 12]. Liu et al. found that elevated NT-pro-BNP level is associated with myocardial fibrosis assessed by cardiac MRI T1-mapping in a community-based population [13]. However, the relationship between NT-pro-BNP and multi-parameters on left ventricular remodeling derived from cardiac MRI in patients with PA remains unclear. This study aimed to assess the relationship between left ventricular remodeling parameters of cardiac MRI and NT-pro-BNP in patients with PA. Our results will be helpful in better comprehending the potential role of neurohormone activation in left ventricular remodeling of patients with PA.

Materials and Methods

Study population

Patients diagnosed with PA [14] were prospectively recruited between May 2020 and May 2022. This study was approved by the Ethics Committee of Sichuan University West China Hospital in accordance with the Declaration of Helsinki, as revised in 2013 (IRB No. 2016 355), and is registered in the Chinese Clinical Trial Registry (Registration number: ChiCTR2000031792). Each participant provided written informed consent before enrollment. In this study, mineralocorticoid receptor antagonists and potassium-sparing diuretics were withdrawn 4 weeks before aldosterone-to-renin ratio (ARR) testing. Participants with a plasma ARR ≥ 30, participants with an ARR ≥ 20 while plasma renin activity (PRA) < 1 ng/mL/h and participants with a plasma aldosterone concentration ≥ 15 ng/dL were further evaluated using confirmatory tests. Confirmatory tests included a saline infusion and/or a captopril challenge test. A post-infusion plasma aldosterone concentration of > 10 ng/dL was the cut-off value for PA with the saline infusion test, while a 30 % captopril-induced suppression of plasma aldosterone after the captopril challenge test indicated PA. As a control group, patients with essential hypertension (EH) were also included in this study. EH was defined as systolic blood pressure (SBP) ≥ 140 mmHg or diastolic blood pressure (DBP) ≥ 90 mmHg, while eliminating the possibility of secondary hypertension. The exclusion criteria were: 1) patients aged < 18 years, 2) patients with known cardiovascular disease except for hypertension, such as myocardial infarction, unstable angina, atrial fibrillation, severe arrhythmia, systolic heart failure, cardiomyopathy, and valvular disease, 3) patients with cardioverter defibrillator or pacemaker implantation, 4) patients with any other known chronic disease (including neurological disease, chronic lung disease, diabetes mellitus, cancer, autoimmune disease, etc.), 5) patients with systemic infection, severe trauma, or history of surgery within the past 3 months, 6) patients with claustrophobia or other conditions that could lead to premature scan termination, and 7) patients with artifacts on cardiac MRI. The baseline characteristics, including demographic data, laboratory examination results, and cardiac MRI-derived parameters, were collected. Serum levels of potassium, plasma N-terminal pro-brain natriuretic peptide (NT-pro-BNP), troponin T(TnT), and creatine kinase MB (CK-MB) were measured using standardized equipment by the clinical laboratory. Normal plasma NT-pro-BNP level was defined according to the American College of Cardiology Foundation/American College of Cardiology guidelines for the management of heart failure [15].

Cardiac magnetic resonance imaging acquisition

All subjects underwent cardiac MRI using a 3 T scanner (MAGNETOM Trio A Tim System; Siemens Healthcare, Erlangen, Germany). All the cardiac MRI images were acquired per the standard protocol [16]. The balanced steady-state-free-precession sequence was used to obtain the cine images in short-axis planes from the base of the heart to the apex, and the following scan parameters were used: repeti-

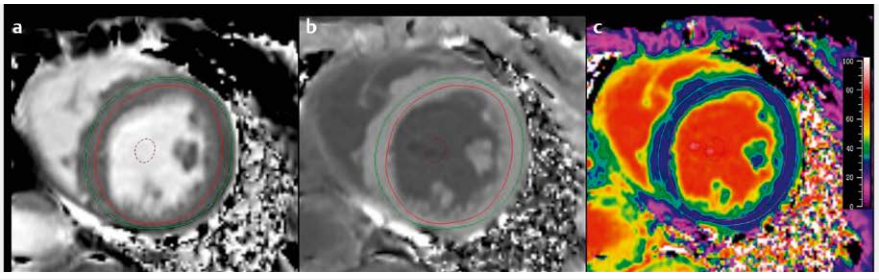

▶ **Fig. 1** Post-processing of T1 mapping in a patient with primary aldosteronism (PA). Endocardial (red circle by solid line) and epicardial contours (green circle by solid line) were traced manually on the pre-contrast (**a**) and post-contrast (**b**) images of a PA patient to calculate native T1 and post T1 values of left ventricular myocardium. For the calculation of extracellular volume (ECV) (**c**), region of interest (ROI) was drawn in the center of the blood pool (red circle by dotted line).

tion time (TR)/echo time (TE), 3.4 ms/1.3 ms; field of view (FOV), 320–360 mm^2; flip angle (FA), 50°; voxel size, 1.4 × 1.3 × 8 mm^3; matrix size, 256 × 144; and thickness, 8 mm with no gap. T1 mapping was obtained using a motion-corrected Modified Look-Locker Inversion (MOLLI) recovery sequence with a scanning scheme of 5b(3b)3b (where b stands for heartbeat) on the mid-ventricular short-axis slice. The parameters for MOLLI were as follows: TR, 2.9 ms; TE, 1.12 ms; total acquisition, 11 heartbeats; in-plane spatial resolution, 2.4 × 1.8 mm; FA, 35 °; bandwidth, 930 Hz/pixel; inversion time (TI) of the first experiment, 100 ms; TI increment, 80 ms; and matrix, 192 × 144. Postcontrast T1 mapping was repeated approximately 15 min after intravenous injection of gadolinium using the same MOLLI sequence (scan scheme: 4b(1b)3b(1b)2b) in the same slice. Hematocrit (HCT) was acquired to calculate the extracellular volume (ECV) within 24 h of cardiac MRI acquisition.

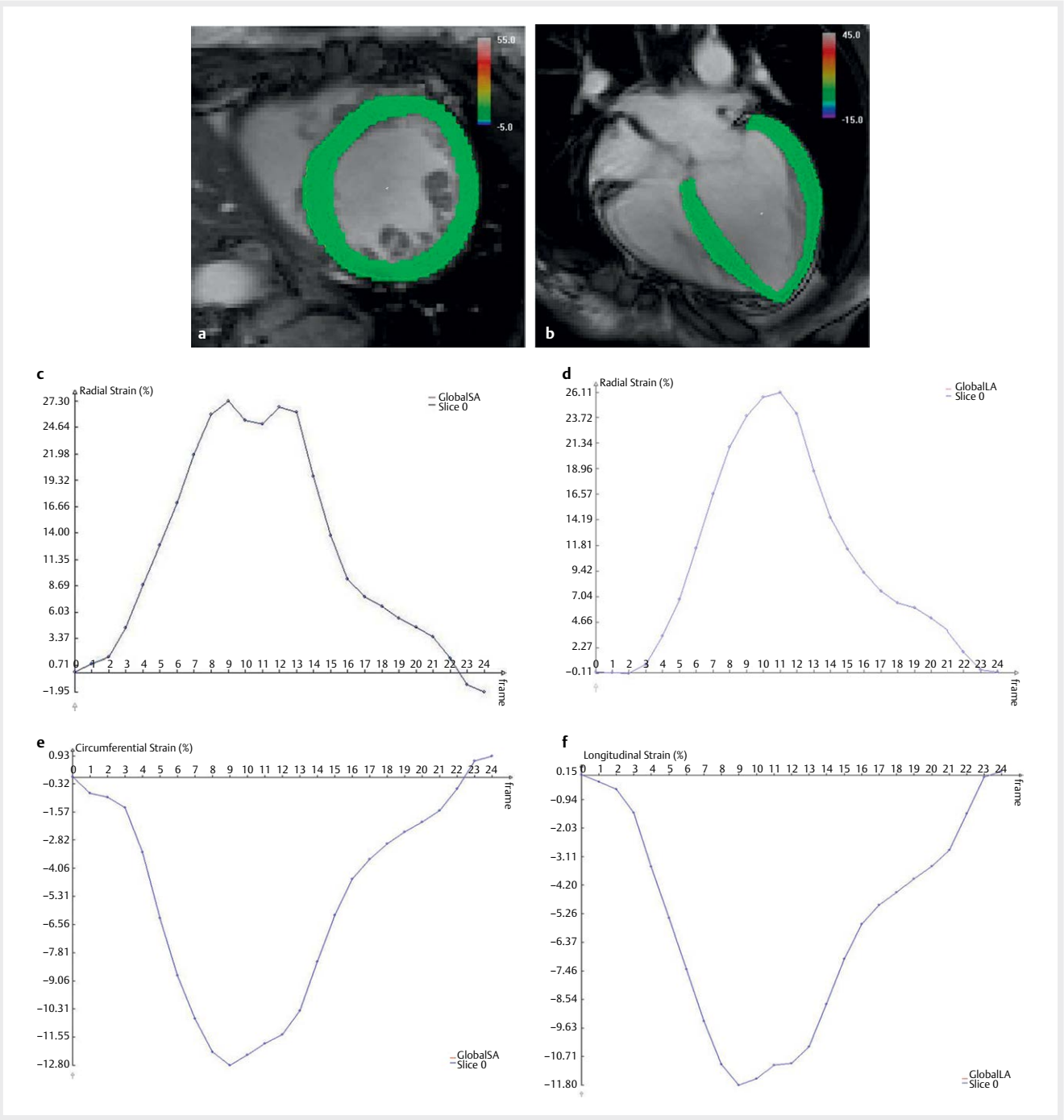

▶ **Fig. 2** Post-processing of feature-tracking in a patient with PA. Left ventricular short-axis global circumferential strain (GCS-sax) and short-axis global radial strain (GRS-sax) were measured in the mid short-axis slice (**a**). Four-chamber global longitudinal strain (GLS-4ch) and four-chamber global radial strain (GRS-4ch) were obtained in the four-chamber slice (**b**). Short-axis global radial strain curve (**c**), short-axis global circumferential strain curve (**e**), four-chamber global radial strain curve (**d**), and four-chamber global radial strain curve (**f**) were also acquired.

Cardiac magnetic resonance imaging analysis

All subjects were analyzed using dedicated software (Argus; Siemens Healthcare, Erlangen, Germany). Two radiologists (each with more than 5 years of experience and 1000 cases) delineated the endocardial and epicardial contours in diastole and systole in a stack of short-axis slices that covered the whole left ventricle. The left ventricular function parameters, including left ventricular end-diastolic volume, left ventricular end-systolic volume, left ventricular ejection fraction, and left ventricular mass, were obtained. Body-surface area indexed values, except left ventricular ejection fraction, were calculated [17].

T1 mapping measurements

Native T1 and ECV were analyzed using the QMass7.6 software (Medis, Leiden, The Netherlands) based on the MOLLI images of mid-ventricular short-axis slice, and the endocardial and epicardial contours were traced manually on the pre- and post-contrast images (▶ **Fig. 1**). For calculating ECV, a region of interest in the center of the blood pool in the pre- and post-contrast T1 map should be drawn, excluding papillary muscles and trabeculae. ECV was calculated as follows [18]:

$$\mathrm{ECV} = (1 - \mathrm{HCT}) \times \frac{1/\mathrm{T1myocardial\ post-contrast} - 1/\mathrm{T1myocardial\ pre-contrast}}{1/\mathrm{T1blood\ post-contrast} - 1/\mathrm{T1blood\ pre-contrast}}$$

Left ventricular myocardial strain

The myocardial strain was quantified using prototype analytic software (TrufiStrain; Siemens Healthcare, Erlangen, Germany) on cine images. The endo- and epicardial contours of the end-diastolic left ventricle were drawn manually, and the contours on the additional cardiac phases were detected automatically (▶ **Fig. 2**). Left ventricular four-chamber global longitudinal strain (GLS-4ch) and four-chamber global radial strain (GRS-4ch) were obtained in the four-chamber slices. Short-axis global circumferential strain (GCS-sax) and short-axis global radial strain (GRS-sax) were measured in the mid-short-axis slices.

Statistical analysis

Statistical analysis was performed using statistical software SPSS 23 (IBM Corporation, Chicago, USA) and GraphPad Prism 6 (GraphPad Software, San Diego, USA). Normally distributed continuous variables were expressed as the mean ± standard deviation, and continuous variables with non-normal distribution were expressed as the median and interquartile range. The categorical variables were expressed as percentages. Differences in continuous variables between two groups were analyzed using Student's *t*-test or Mann–Whitney U test. Differences in categorical variables between two groups were analyzed by chi-squared test. Spearman's correlation and linear regression were used to analyze the relationships between left ventricular remodeling parameters and plasma NT-pro-BNP level. Variables with $P < 0.05$ on univariable regressions were included in the multivariable regression analysis. Variables independently related to left ventricular remodeling parameters were selected in a step-wise method. $P < 0.05$ was considered as statistically significant.

Results

Clinical Characteristics

A total of 74 patients with PA and 39 patients with EH were included in this study. The clinical characteristics of patients with PA are presented in ▶ **Table 1**, while the clinical characteristics of patients with EH are presented in **Supplementary Table 1**. With essentially the same baseline level of gender, age, BMI, blood pressure, and high blood pressure history, patients with PA demonstrated higher NT-pro-BNP level than patients with EH. Patients with abnormal

▶ **Table 1** Clinical Characteristics of Patients with Normal and with Abnormal Plasma NT-pro BNP level.

	Overall (N = 74)	Normal (N = 59)	Abnormal (N = 15)	P
Male (%)	24 (32.4)	17 (28.8)	7 (46.7)	0.312
Age (years)	47.0 ± 11.7	48.1 ± 11.9	42.8 ± 10.5	0.118
BMI (kg/m2)	24.8 ± 3.6	25.2 ± 3.6	23.1 ± 3.4	0.045
SBP (mmHg)	146 ± 17	146 ± 16	147 ± 23	0.833
DBP (mmHg)	94 ± 12	94 ± 12	96 ± 11	0.583
HR (min^{-1})	76 ± 11	78 ± 10	71 ± 11	0.014
HCT (%)	41.0 (38.0~43.0)	41.0 (38.5~43.0)	38.0 (33.5~42.0)	0.039
Serum potassium (mmol/L)	3.5 (3.1~3.9)	3.6 (3.1~3.9)	3.2 (2.9~3.7)	0.170
Ald (ng/dL)	29.1 (21.9~41.0)	28.5 (22.0~38.9)	38.9 (23.0~45.6)	0.259
PRA (ng/mL/h)	0.2 (0.0~0.5)	0.3 (0.1~0.6)	0.0 (0.0~0.3)	0.010
ARR	113.0 (49.9~534.9)	101.1 (45.2~381.3)	498.6 (127.0~955.8)	0.011
NT-proBNP (pg/mL)	86.0 (49.5~145.5)	70.0(42.0~96.5)	232.0(159.5~372.0)	<0.001
hsTnT (ng/L)	6.5 (3.8~9.7)	5.3 (3.5~8.9)	8.0 (6.6~10.8)	0.015
CKMB (ng/mL)	1.1 (0.8~1.4)	1.1 (0.8~1.3)	1.2 (0.7~1.7)	0.481
HBP history (months)	36 (12–114)	36 (11–96)	48 (12–120)	0.666

BMI, body mass index; SBP, systolic blood pressure; DBP, diastolic blood pressure; HR: heart rate; HCT: Hematocrit; Ald, aldosterone; PRA, plasma renin activity; ARR, aldosterone-to-renin ratio; NT-pro BNP, N-terminal pro-brain natriuretic peptide; hsTnT: high sensitivity troponin T; CKMB, creatine kinase MB type; HBP: high blood pressure.

NT-pro-BNP level had lower BMI, HR, HCT, and PRA and higher hsTnT and ARR than those with normal NT-pro-BNP.

Left ventricular remodeling parameters in patients with primary aldosteronism and essential hypertension

Comparisons of left ventricular remodeling parameters between patients with PA and EH are presented in **Supplementary Figure 1**. Patients with PA demonstrated higher native T1 level than patients with EH (1227 ± 41 vs. 1206 ± 43 ms, P = 0.015). Comparisons of left ventricular remodeling parameters between patients with normal and abnormal NT-pro-BNP levels are presented in ▶ **Fig. 3**. Compared with normal NT-pro-BNP patients, patients with PA having abnormal NT-pro-BNP had higher left ventricular end-diastolic volume index (LVEDVi) (79.7 ± 12.6 vs. 93.8 ± 20.2 mL/m^2, P = 0.001); left ventricular end-systolic volume index (LVESVi) (32.4 ± 9.0 vs. 44.3 ± 15.1 mL/m^2, P < 0.001); left ventricular mass index (LVmassi) (56.1 ± 13.2 vs. 76.3 ± 21.2 g/m^2, P < 0.001); ECV (26.4 ± 2.8 vs. 28.2 ± 4.2 %, P = 0.045); short-axis global circumferential strain (GCS-sax) [(−15.5 ± 2.6) vs. (−12.6 ± 2.8) %, P < 0.001]; and four-chamber global longitudinal strain (GLS-4ch) [(−14.0 ± 2.7) vs. (−12.1 ± 1.5) %, P = 0.011] and lower left ventricular ejection fraction (LVEF) [(59.7 ± 7.6) vs. (53.6 ± 8.8) %, P = 0.008]; short-axis global radial strain (GRS-sax) (46.1 ± 10.4 vs. 37.0 ± 10.4 %, P = 0.003); and four-

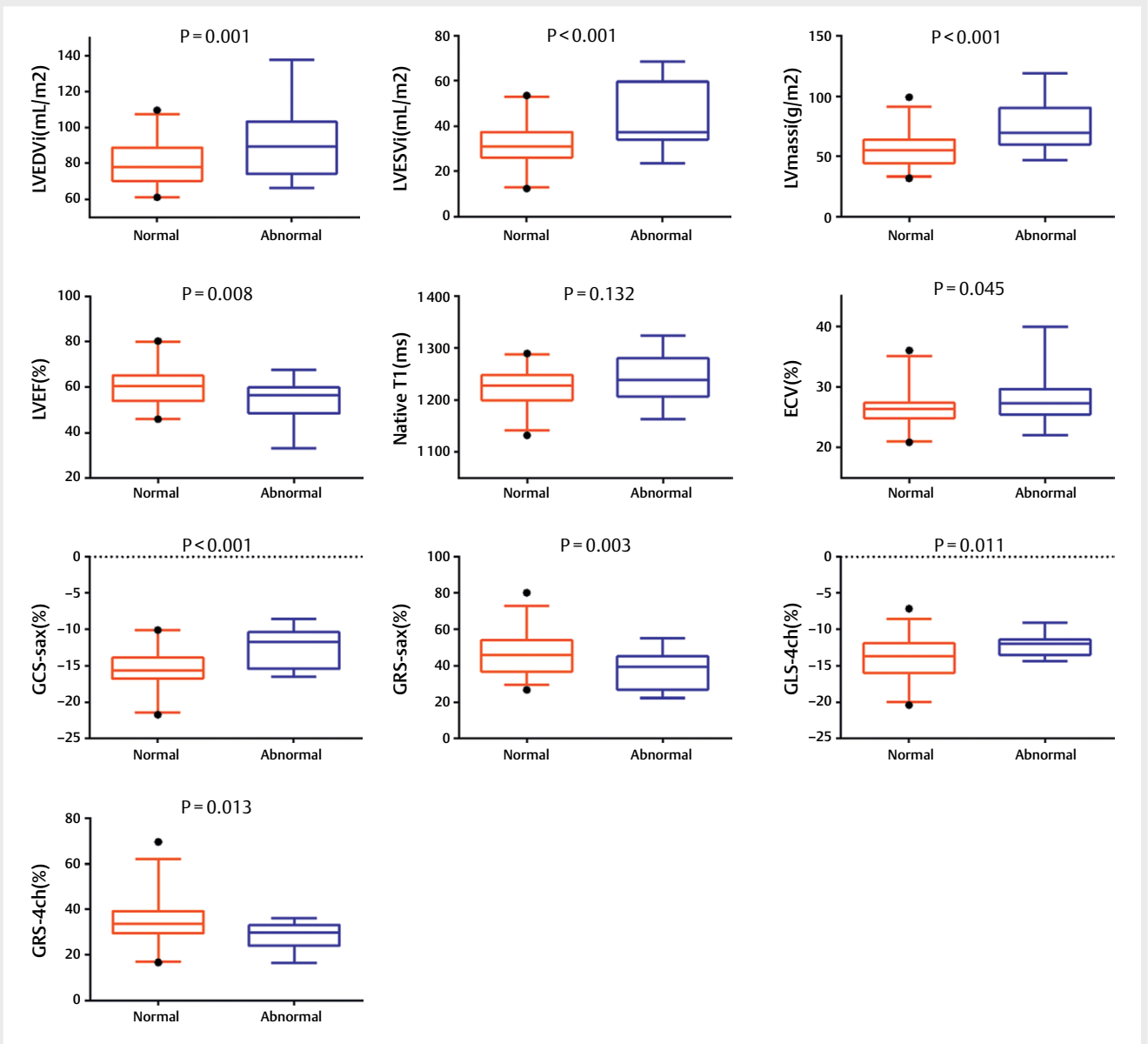

▶ **Fig. 3** Comparison of CMR left ventricular remodeling parameters between patients with different plasma NT-pro BNP level. Box represents the quartile of data. Line inside the box represents the median of data, and the whisker represents the 95 % confidence interval. Points outside the whisker represents the data outside the 95 % confidence interval. CMR: cardiac magnetic resonance; LVEDVi, left ventricular end-diastolic volume index; LVESVi, left ventricular end-systolic volume index; LVmassi, left ventricular mass index; LVEF, left ventricular ejection fraction; ECV, extracellular volume; GCS, global circumferential strain; GRS, global radial strain; GLS, global longitudinal strain; sax: short axis; 4ch: 4 chambers.

▶ **Table 2** Spearman's Correlations Between NT-pro BNP and Left Ventricular Remodeling Parameters.

	r	P
LVEDVi(mL/m^2)	0.315	0.006
LVESVi(mL/m^2)	0.313	0.007
LVmassi(g/m^2)	0.313	0.007
LVEF(%)	−0.171	0.145
Native T1(ms)	0.266	0.022
ECV(%)	0.375	0.001
GCS-sax(%)	0.241	0.039
GRS-sax(%)	−0.151	0.199
GLS-4ch(%)	0.250	0.032
GRS-4ch(%)	−0.323	0.005

LVEDVi, left ventricular end-diastolic volume index; LVESVi, left ventricular end-systolic volume index; LVmassi, left ventricular mass index; LVEF, left ventricular ejection fraction; ECV, extracellular volume; GCS, global circumferential strain; GRS, global radial strain; GLS, global longitudinal strain; sax: short axis; 4ch: 4 chambers.

chamber global radial strain (GRS-4ch) (35.1 ± 9.0 vs. 28.9 ± 5.4 %, P = 0.013).

Relationship between NT-pro-BNP and left ventricle remodeling parameters

Spearman's correlation between NT-pro-BNP and left ventricle remodeling parameters are shown in ▶ **Table 2**. LVEDVi, LVESVi, LVmassi, native T1, ECV, GCS-sax, GLS-4ch, and GRS-4ch were significantly related to the plasma NT-pro-BNP level.

Univariable and multivariable linear regression analysis was performed to determine the factors influencing the left ventricle remodeling parameters significantly related to plasma NT-pro-BNP level (▶ **Table 3** , **Supplementary Table 2**, and **Supplementary Table 3**). After adjusting the statistically significant variables in univariable linear regression analysis (P < 0.05), plasma NT-pro-BNP level was independently related to LVEDVi, LVESVi, LVmassi, native T1, ECV, GCS-sax, GLS-4ch, and GRS-4ch.

Discussion

In this study, we found that 1) patients with PA demonstrated higher NT-pro-BNP and native T1 level than patients with EH, 2) patients with PA with abnormal plasma NT-pro-BNP level showed different left ventricular remodeling parameters, including left ventricular function, strain, and T1 mapping parameters when compared with PA patients with normal plasma NT-pro-BNP level, and 3) plasma NT-pro-BNP level was also independently related to left ventricular remodeling parameters, including LVEDVi, LVESVi, LVmassi, native T1, ECV, GCS-sax, GLS-4ch, and GRS-4ch in patients with PA.

NT-pro-BNP is generated along with BNP in response to the increased atrial and ventricular wall stress [19, 20]. Increasing wall stress, as a result of increasing pre- or after-load in the heart, is related to ventricular remodeling. Breetveld et al. found that increased pressure load was related to concentric left ventricular remodeling in patients with preeclampsia [21]. Chen et al. found that left ventricular after-load, demonstrated by blood pressure, was related to wall thickness and LVmassi in an Asian asymptomatic cohort [22]. This could explain the phenomenon that plasma NT-pro-BNP level was related to left ventricular remodeling parameters.

Some clinical studies support our results and reveal the relationship between NT-pro-BNP and left ventricle remodeling. In the PROVE-HF study, reduction of NT-pro-BNP was correlated with left ventricle remodeling parameters, represented by a decrease in left ventricle volume and an increase in ejection fraction measured by echocardiography during the one-year follow-up in patients with heart failure with reduced ejection fraction (HFrEF) treated by sacubitril-valsartan [23]. The EVALUATE-HF study reached a similar conclusion that NT-pro-BNP was negatively correlated with the decrease of left ventricle volume derived from echocardiography after 12-week treatment of sacubitril-valsartan in patients with HFrEF [24]. Furthermore, in a study from the Multi-Ethnic Study of Atherosclerosis (MESA) cohort, NT-pro-BNP was related to native T1 and ECV derived from cardiac MRI, showing that elevation of NT-pro-BNP was an indicator of subclinical left ventricle fibrosis, which was a sign of early left ventricle remodeling [13].

However, these studies were not tailored to patients with PA. Our study is specific to patients with PA and has comprehensively measured the left ventricle remodeling parameters, including indices of left ventricle volume, function, tissue characteristics, and strain. Little was known about the role that NT-pro-BNP plays in patients with PA. Jakubik et al. found that BNP in patients with PA or EH did not show significant differences, but BNP in both patients with PA and EH was higher than in healthy controls [25]. Kato et al. found that BNP is related to cardiac load or volume retention in patients with PA due to adrenal adenoma [26]. In this study, the BNP level was independently related to T1 mapping and feature tracking parameters, which could be measured by native T1, ECV, and ventricular strain. These parameters were proven to be imaging markers of early left ventricular remodeling parameters [27–32]. To our knowledge, this is the first study to analyze the correlation between NT-pro-BNP and early left ventricular remodeling parameters on cardiac MRI. The results suggested that doctors should pay attention to the NT-pro-BNP level in patients with PA to be alert to early left ventricular remodeling and perform timely intervention. Regular follow-up of NT-pro-BNP levels in patients with PA might be necessary. However, this study does not describe the relationship between NT-pro-BNP and follow-up outcomes of cardiac MRI-derived left ventricular remodeling indicators.

Our study has some limitations. First, the sample size of our study was relatively small, which limited the application value of this study. Thus, future studies with larger sample sizes are needed. Second, this was a cross-sectional study. The results of this study only reflected the relationship between baseline plasma NT-pro-BNP level and baseline left ventricular remodeling parameters, and we did not conduct a follow-up cardiac MRI in these patients with PA. The follow-up of these patients is needed to evaluate the relationship between baseline plasma NT-pro-BNP level and change of the cardiac MRI-derived left ventricular remodeling parameters, which could more intuitively reflect the phenomenon of left ventricular remodeling than baseline left ventricular remodeling parameters.

▲ **Table 3** Linear Regression Analysis between Left Ventricular Volume and Mass Parameters and Plasma NT-pro BNP Level.

	LVEDVi (mL/m²) (R² = 0.454)				LVESVi (mL/m²) (R² = 0.448)				LVmassi (g/m²) (R² = 0.423)			
	Univariable		Multivariable		Univariable		Multivariable		Univariable		Multivariable	
	β	P	β	P	β	P	β	P	β	P	β	P
Male	0.262	0.024	0.266	0.004	0.164	0.164			0.415	<0.001	0.421	<0.001
Age (years)	−0.201	0.086			−0.171	0.144			−0.231	0.048	−0.190	0.052
BMI (kg/m2)	0.104	0.379			0.119	0.311			0.107	0.364		
SBP (mmHg)	0.233	0.047	0.031	0.750	0.162	0.171			0.274	0.046		
DBP (mmHg)	0.155	0.190			0.118	0.318			0.173	0.043		
HR (min^{-1})	−0.175	0.135			−0.062	0.600			−0.184	0.117		
Serum potassium (mmol/L)	−0.280	0.016	−0.081	0.458	−0.187	0.111			−0.299	0.010		
Ald (ng/dL)	0.292	0.012	0.202	0.030	0.251	0.031	0.209	0.024	0.230	0.049		
PRA (ng/mL/h)	−0.219	0.060			−0.177	0.132			−0.177	0.130		
NT-pro BNP (pg/mL)	0.441	<0.001	0.306	0.003	0.570	<0.001	0.445	<0.001	0.388	0.001	0.322	0.003
hsTnT (ng/L)	0.345	0.003	−0.117	0.324	0.341	0.004	0.053	0.604	0.459	<0.001		
CKMB (ng/mL)	0.566	<0.001	0.403	<0.001	0.529	<0.001	0.309	0.003	0.358	0.001	0.289	0.007
HBP history (months)	−0.067	0.568			−0.041	0.732			−0.104	0.378		

BMI, body mass index; SBP, systolic blood pressure; DBP, diastolic blood pressure; HR: heart rate; Ald, aldosterone; PRA, plasma renin activity; NT-pro BNP, N-terminal pro-brain natriuretic peptide; hsTnT: high sensitivity troponin T; CKMB, creatine kinase MB type; HBP: high blood pressure; LVEDVi, left ventricular end-diastolic volume index; LVESVi, left ventricular end-systolic volume index; LVmassi, left ventricular mass index Variables with P < 0.05 on univariable regressions were included in the multivariable regression analysis R^2, adjusted R^2 value of the multivariable linear regression model.

Conclusions

In this study, we found the relationship between plasma NT-pro-BNP level and left ventricular remodeling parameters derived from cardiac MRI in patients with PA. This result implied that in routine clinical assessment, clinicians should pay attention to NT-pro-BNP assessment in patients with PA.

Author contribution statement

Tao Wu and Chenxiao Xu contributed equally to the study design, data analysis and interpretation, statistical analysis, and manuscript drafting. Jiayu Sun and Yan Ren are the supervisors of this study and contributed to the study design, preparation, editing, and review of the final manuscript. Lu Tang collected clinical data. Yucheng Chen contributed to the study design and helped revise the manuscript. Xi Wu, Xun Yue, and Pengfei Peng analyzed the imaging data. Wei Cheng, Shuai He, and Lei Li carried out subject scanning and performed data analysis and interpretation. All the authors read and approved the final manuscript.

Funding

This work was supported by grants from the Key R & D Projects in Sichuan Province (No. 2020YFS0123) and 1 · 3 · 5 Project for Disciplines of Excellence–Clinical Research Incubation Project (2018HXFH009).

Conflict of Interest

There is no conflict of interest that could be perceived as prejudicing the impartiality of the research reported.

References

[1] Reincke M, Bancos I, Mulatero P et al. Diagnosis and treatment of primary aldosteronism. Lancet Diabetes Endocrinol 2021; 9: 876–892. DOI: 10.1016/s2213-8587(21)00210-2

[2] Zennaro MC, Boulkroun S, Fernandes-Rosa FL. Pathogenesis and treatment of primary aldosteronism. Nat Rev Endocrinol 2020; 16: 578–589. DOI: 10.1038/s41574-020-0382-4

[3] Cesari M, Letizia C, Angeli P et al. Cardiac remodeling in patients with primary and secondary aldosteronism: A tissue Doppler study. Circ Cardiovasc Imaging 2016; 9:. DOI: 10.1161/circimaging.116.004815

[4] Bière L, Donal E, Jacquier A et al. A new look at left ventricular remodeling definition by cardiac imaging. Int J Cardiol 2016; 209: 17–19. DOI: 10.1016/j.ijcard.2016.02.009

[5] Wu T, Ren Y, Wang W et al. Left Ventricular remodeling in patients with primary aldosteronism: A prospective cardiac magnetic resonance imaging study. Korean J Radiol 2021; 22: 1619–1627. DOI: 10.3348/kjr.2020.1291

[6] Tsai CH, Pan CT, Chang YY et al. Left ventricular remodeling and dysfunction in primary aldosteronism. J Hum Hypertens 2021; 35: 131–147. DOI: 10.1038/s41371-020-00426-y

[7] Rossi GP, Cesari M, Cuspidi C et al. Long-term control of arterial hypertension and regression of left ventricular hypertrophy with treatment of primary aldosteronism. Hypertension 2013; 62: 62–69. DOI: 10.1161/hypertensionaha.113.01316

[8] Gastl M, Behm P, Haberkorn S et al. Role of T2 mapping in left ventricular reverse remodeling after TAVR. Int J Cardiol 2018; 266: 262–268. DOI: 10.1016/j.ijcard.2018.02.029

[9] Nordin S, Dancy L, Moon JC et al. Clinical applications of multiparametric CMR in left ventricular hypertrophy. Int J Cardiovasc Imaging 2018; 34: 577–585. DOI: 10.1007/s10554-018-1320-6

[10] Tian H, Cui J, Yang C et al. Left ventricular remodeling in hypertrophic cardiomyopathy patients with atrial fibrillation. BMC Cardiovasc Disord 2018; 18: 207. DOI: 10.1186/s12872-018-0945-7

[11] Hall C. Essential biochemistry and physiology of (NT-pro)BNP. Eur J Heart Fail 2004; 6: 257–260. DOI: 10.1016/j.ejheart.2003.12.015

[12] Whitman IR, Vittinghoff E, DeFilippi CR et al. NT-pro BNP as a mediator of the racial difference in incident atrial fibrillation and heart failure. J Am Heart Assoc 2019; 8: e010868. DOI: 10.1161/jaha.118.010868

[13] Liu CY, Heckbert SR, Lai S et al. Association of elevated NT-proBNP with myocardial fibrosis in the Multi-Ethnic Study of Atherosclerosis (MESA). J Am Coll Cardiol 2017; 70: 3102–3109. DOI: 10.1016/j.jacc.2017.10.044

[14] Funder JW, Carey RM, Mantero F et al. The management of primary aldosteronism: Case detection, diagnosis, and treatment: An Endocrine Society Clinical Practice Guideline. J Clin Endocrinol Metab 2016; 101: 1889–1916. DOI: 10.1210/jc.2015-4061

[15] Yancy CW, Jessup M, Bozkurt B et al. 2017 ACC/AHA/HFSA focused update of the 2013 ACCF/AHA guideline for the management of heart failure: A Report of the American College of Cardiology/American Heart Association Task Force on Clinical Practice Guidelines and the Heart Failure Society of America. Circulation 2017; 136: e137–e161. DOI: 10.1161/cir.0000000000000509

[16] Kramer CM, Barkhausen J, Bucciarelli-Ducci C et al. Standardized cardiovascular magnetic resonance imaging (CMR) protocols: 2020 update. J Cardiovasc Magn Reson 2020; 22: 17. DOI: 10.1186/s12968-020-00607-1

[17] Meloni A, Righi R, Missere M et al. Biventricular reference values by body surface area, age, and gender in a large cohort of well-treated thalassemia major patients without heart damage using a multiparametric CMR approach. J Magn Reson Imag 2021; 53: 61–70. DOI: 10.1002/jmri.27169

[18] Chen CA, Dusenbery SM, Valente AM et al. Myocardial ECV fraction assessed by CMR is associated with type of hemodynamic load and arrhythmia in repaired tetralogy of fallot. JACC Cardiovasc Imag 2016; 9: 1–10. DOI: 10.1016/j.jcmg.2015.09.011

[19] Goetze JP, Bruneau BG, Ramos HR et al. Cardiac natriuretic peptides. Nat Rev Cardiol 2020; 17: 698–717. DOI: 10.1038/s41569-020-0381-0

[20] Wu L, Zhang L, Ai Z et al. Association between risk factors and left ventricular remodeling in middle-aged and aged population: A community-based study. J Hypertens 2012; 30: 1862–1873. DOI: 10.1097/HJH.0b013e3283563418

[21] Breetveld NM, Alers RJ, Geerts L et al. Low plasma volume and increased pressure load relate to concentric left ventricular remodeling after preeclampsia: A longitudinal study. J Am Heart Assoc 2020; 9: e015043. DOI: 10.1161/jaha.119.015043

[22] Chen C, Sung KT, Shih SC et al. Age, Gender and load-related influences on left ventricular geometric remodeling, systolic mid-wall function, and NT-proBNP in asymptomatic Asian population. PloS One 2016; 11: e0156467. DOI: 10.1371/journal.pone.0156467

[23] Januzzi JL Jr., Prescott MF, Butler J et al. Association of change in N-terminal pro-B-type natriuretic peptide following initiation of sacubitril-valsartan treatment with cardiac structure and function in patients with heart failure with reduced ejection fraction. JAMA 2019; 322: 1085–1095. DOI: 10.1001/jama.2019.12821

[24] Desai AS, Solomon SD, Shah AM et al. Effect of sacubitril-valsartan vs enalapril on aortic stiffness in patients with heart failure and reduced ejection fraction: A randomized clinical trial. JAMA 2019; 322: 1077–1084. DOI: 10.1001/jama.2019.12843

[25] Jakubik P, Janota T, Widimsky J Jr. et al. Impact of essential hypertension and primary aldosteronism on plasma brain natriuretic peptide concentration. Blood Press 2006; 15: 302–307. DOI: 10.1080/08037050601037760

[26] Kato J, Etoh T, Kitamura K et al. Atrial and brain natriuretic peptides as markers of cardiac load and volume retention in primary aldosteronism. Am J Hypertens 2005; 18: 354–357. DOI: 10.1016/j.amjhyper.2004.09.016

[27] Zhang G, Shi K, Yan WF et al. Effects of diabetes mellitus on left ventricular function and remodeling in hypertensive patients with heart failure with reduced ejection fraction: Assessment with 3.0 T MRI feature tracking. Cardiovasc Diabetol 2022; 21: 69. DOI: 10.1186/s12933-022-01504-w

[28] Kramer CM, Chandrashekhar Y, Narula J. The tissue issue: T1 mapping and the myocardium. JACC Cardiovascular Imaging 2016; 9: 88–90. DOI: 10.1016/j.jcmg.2015.11.003

[29] Wei X, Jian X, Xie J et al. T1 mapping and feature tracking imaging of left ventricular extracellular remodeling in severe aortic stenosis. Cardiovasc Diagn Ther 2020; 10: 1847–1857. DOI: 10.21037/cdt-20-803

[30] Yang MX, He Y, Ma M et al. Characterization of infarcted myocardium by T1-mapping and its association with left ventricular remodeling. Eur J Radiol 2021; 137: 109590. DOI: 10.1016/j.ejrad.2021.109590

[31] Rank N, Stoiber L, Nasser M et al. Assessment of 10-year left-ventricular-remodeling by CMR in patients following aortic valve replacement. Front Cardiovasc Med 2021; 8: 645693. DOI: 10.3389/fcvm.2021.645693

[32] Reindl M, Tiller C, Holzknecht M et al. Global longitudinal strain by feature tracking for optimized prediction of adverse remodeling after ST-elevation myocardial infarction. Clin Res Cardiol 2021; 110: 61–71. DOI: 10.1007/s00392-020-01649-2